Comparison of three TCC calculation algorithms for partially coherent imaging simulation

Xiaofei WU [a], Shiyuan LIU [*, b], Wei LIU [a], Tingting ZHOU [b], and Lijuan WANG [b]

[a] Wuhan National Laboratory for Optoelectronics, Huazhong University of Science and Technology, Wuhan 430074, China

[b] State Key Laboratory of Digital Manufacturing Equipment and Technology, Huazhong University of Science and Technology, Wuhan 430074, China

ABSTRACT

Three kinds of TCC (transmission cross coefficient) calculation algorithms used for partially coherent imaging simulation, including the integration algorithm, the analytical algorithm, and the matrix-based fast algorithm, are reviewed for their rigorous formulations and numerical implementations. The accuracy and speed achievable using these algorithms are compared by simulations conducted on several mainstream illumination sources commonly used in current lithographic tools. Simulation results demonstrate that the integration algorithm is quite accurate but time consuming, while the matrix-based fast algorithm is efficient but its accuracy is heavily dependent on simulation resolution. The analytical algorithm is both efficient and accurate but not suitable for arbitrary optical systems. It is therefore concluded that each TCC calculation algorithm has its pros and cons with a compromise necessary to achieve a balance between accuracy and speed. The observations are useful in fast lithographic simulation for aerial image modeling, optical proximity correction (OPC), source mask optimization (SMO), and critical dimension (CD) prediction.

Keywords: lithographic simulation, transmission cross coefficient, partial coherent imaging, Fourier transform

1. INTRODUCTION

The imaging process in optical lithography is modeled as a pupil function with a partially coherent illumination source, namely the partially coherent system. The theories of aerial image formation process of this kind of system can be roughly classified into two categories: one follows Abbe's theory and the other Hopkins' theory [1-3]. Both of these two theories regard the system as a set of mutually incoherent point sources, and the whole intensity distribution on the image plane is the superimposition of the intensities formed by all of the point sources. In Abbe's theory, the aerial image is calculated directly by the summation of all point sources, and for each of them the Fourier transform (FT) is needed. The computation speed of Abbe's method is thus limited by the repetition of the fast Fourier transform (FFT). On the other hand, in Hopkins' theory, the transmission cross coefficient (TCC) matrix is introduced as a combination of the source and pupil. It is possible to use fewer kernels to speed up the aerial image calculation due to the concept of sum of coherent systems (SOCS) [4-5].

The TCC matrix based on Hopkins' theory is basically a four-dimensional (4D) matrix, which is the double integral of the aperture and two offset pupil functions. The calculation of this matrix is a key step of aerial image formation but is computationally costly and time consuming especially for high resolution simulation. It is also known that for a given imaging system the TCC matrix can be calculated in advance only once, and the aerial image for any mask can be then calculated by the product of TCC with the mask spectrum [5]. Therefore, the TCC matrix has wide applications in fast lithographic simulation, and it is highly desirable to develop TCC algorithms not only with high accuracy but also with less expensive computation.

There are several kinds of TCC calculation algorithms in the history of lithographic simulation, which can be categorized as the integration algorithm, the analytical algorithm, and the matrix-based fast algorithm. The traditional integration algorithm utilized a double integral over the intersection region of three circles, namely the source and two offset pupils. The analytical algorithm is quite efficient and accurate and is a key step for analytical aerial image formation. It was first proposed by Kintner for one-dimensional (1D) masks with circular aperture and aberration-free optics [6]. Subramanian

* Contact author: shyliu@mail.hust.edu.cn; phone: +86 27 87792409; fax: +86 27 87792413.

Sixth International Symposium on Precision Engineering Measurements and Instrumentation, edited by Jiubin Tan, Xianfang Wen, Proc. of SPIE Vol. 7544, 75440Z · © 2010 SPIE · CCC code: 0277-786X/10/$18 · doi: 10.1117/12.885227

extended this algorithm so that the defocused image with square pupil can also be supported [7]. Gordon developed an analytical algorithm for 4D TCC calculation through geometrical transform and contour integration by enumerating 18 unique geometrical configurations. He also extended this method to the defocus image so that the simulation of optical lithography becomes a memory limited problem rather than a time limited one [8-9]. Most recently, Kenji reported a matrix-based fast algorithm for TCC calculation according to Abbe's theory. He introduced a matrix known as a pupil shift matrix, and proved that the TCC matrix is simply a product of the pupil shift matrix and its Hermitian conjugate [10]. Roderick Köhle provided another matrix-based algorithm based on the two-dimensional (2D) Fourier transform to calculate TCC since TCC is a generalized convolution in frequency domain [11]. He also applied a polyphase decomposition method to perform decimation which leads to a faster speed for bitmap apertures.

In this paper, three kinds of TCC calculation algorithms used for partially coherent imaging simulation, including the integration algorithm, the analytical algorithm, and the matrix-based fast algorithm, are reviewed for their rigorous formulation and numerical implementation. The accuracy and speed achievable using these algorithms will be compared by simulations for several mainstream illumination sources commonly used in current lithographic tools. The remaining parts of this paper are organized as follows. In section 2, we introduce the partially coherent imaging theory based on Hopkins' theory, and then the rigorous formulation and physical interpretation for three algorithms for TCC calculation will be presented in section 3, respectively. In section 4, the simulation results of these algorithms are performed on the mainstream illumination sources commonly used in current lithographic tools, and the simulation speed and accuracy are compared and discussed in detail. The conclusions based on our work will be provided in section 5.

2. TCC CALCULATION ALGORITHMS

2.1 Transmission cross coefficient

As shown in Figure 1, the elements of a modern optical lithography system can be simplified as an extended source, a condenser lens, an object, projection optics, and an image on the wafer plane.

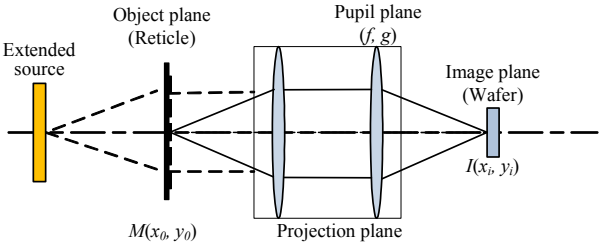

Figure 1. The elements of a modern optical lithographic system

Based on Abbe's theory, the aerial image of the system can be simulated as the summation of all the source points of the illumination. For each source point, the optics is described as a linear system, and the electrical field $E(x, y)$ on the wafer plane can be expressed as [4, 12-13]

$$E(x_i, y_i; f_c, g_c) = \iint O(f - f_c, g - g_c) H(f, g) \exp[-i2\pi(fx + gy)] df dg \tag{1}$$

The intensity on the image plane is proportional to the square magnitude of the electric field distribution and takes the form of

$$I(x_i, y_i) = \iint A(f_c, g_c) \, | \, FT[O(f - f_c, g - g_c) H(f, g)] \, |^2 \, df_c dg_c \tag{2}$$

where $I(x_i, y_i)$ is the aerial image intensity, $A(f_c, g_c)$ is the extended source, $O(f, g)$ is the mask spectrum equal to the Fourier transform (FT) of the $M(x_0, y_0)$, $H(f, g)$ is the pupil. All of the coordinates are normalized so that the cut-off frequency of the pupil plane is the unit.

By interchanging the order of integration, we can express equation (2) according to Hopkins' formulation [2]:

$$I(x_i, y_i) = \iint TCC(f', g'; f'', g'') O(f', g') O^*(f'', g'') \exp[-i2\pi(f' - f'')x - i2\pi(g' - g'')y] df' dg' df'' dg'' \tag{3}$$

Here, TCC is the transmission cross coefficient matrix expressed as

$$TCC(f',g';f'',g'') = \iint A(f_c,g_c)H(f'+f_c,g'+g_c)H^*(f''+f_c,g''+g_c)df_c dg_c \tag{4}$$

For ideal conventional illumination with partially coherent factor σ, the illumination source is a circular function and can be represented as

$$A(f_c,g_c) = circ(\frac{\sqrt{f_c^2+g_c^2}}{\sigma}) \tag{5}$$

The pupil function includes all the information of the aberration and defocus information of the optical systems. For an ideal in-focus system without aberration, the pupil function can be simplified to a circular function similar to the conventional source. In other situations, the aberration of the optics can be represented by a polynomial $W(f, g)$ with 37 Zernike terms, and the pupil function can be written as

$$H(f,g) = circ(\sqrt{f_c^2+g_c^2})\exp[-jkW(f,g)] \tag{6}$$

The TCC matrix is the integration of the source and two offset pupil functions. The value of TCC is zero when there is no intersection region over the three functions. The source function is fixed at the origin of the axis. If the pupil function moves out and is not joined with the source, or the two pupil functions have no overlap area, the value of TCC equals to zero, which can be represented as

$$\begin{aligned} &\left|f'^2+g'^2\right| \le (1+\sigma)^2, \left|f''^2+g''^2\right| \le (1+\sigma)^2 \\ &\left|(f'-f'')^2+(g'-g'')^2\right| \le 4 \end{aligned} \tag{7}$$

The coordinates of the two offset pupils (f', g') and (f'', g'') are the same as that of the TCC and correspond to the diffraction orders of the mask. The TCC matrix is a 4D matrix and the size depends on the resolution of the mask diffraction orders needed in aerial simulation. In addition, the TCC is symmetrical and Hermitian and these characteristics can be exploited in simplification for TCC computation. The calculation of the matrix becomes very time consuming for high resolution because the integration has to be performed for quite a few times.

2.2 Integration algorithm

The traditional integration algorithm utilized a double integral over the intersection region of the source and two offset pupil functions to calculate the TCC matrix. For optics with conventional illumination source, all of these three functions are circular and the radius of the source is the partial coherent factor σ, while that of the pupil is the unit after normalization. The intersection region is shown in Figure 2, where coordinates of two offset pupils are (f', g') and (f'', g'') corresponding to $TCC(f', g'; f'', g'')$. The boundary of the intersection region is made up of several circular arcs which are difficult to describe analytically since the two pupil functions move in two axes. While the boundary of the integration is defined by the three circles, the integrand is determined by the value of the two offset pupils for a binary source, and can be represented as

$$TCC\_integrand = \exp\left[-jkW\left(f_c+f',g_c+g'\right)\right]\exp\left[-jkW\left(f_c+f'',g_c+g''\right)\right] \tag{8}$$

For aerial image calculation with 1D masks, in which the transmission changes in only one direction, only 1D information of the TCC matrix is needed. So TCC becomes a 2D matrix, and the circular arcs can be described analytically. In most cases however, there is no analytical expression of the integration, so we have to use numerical algorithm to perform the integration.

In the numerical integration algorithm, the integration region is divided into a number of rectangular grids and approximates the integration by the sum of the integrand values on all the grids. Problems may occur when the boundary of the region cannot map into a straight line, which is just the case as that occurs in the TCC integration. We can use a smaller grid size to approximate the integration more accurately, with the speed of integration decreased at the same time. So the accuracy of this method is heavily coupled with the resolution of source and diffraction orders needed for aerial image formation. We can also use the numerical integration in the Matlab toolbox to deal with this process, where

smaller grids are used in the places where rectangles cannot map the boundary very well. This algorithm calculates each value of the TCC matrix one by one. For aerial image calculation with N orders of mask spectrum, the integration has to be performed N^2 times for 1D masks with 2D TCC, and N^4 times for 2D masks with 4D TCC. Surely we can exploit the symmetrical characteristic to reduce the evaluation times of the integration, so that the speed of this algorithm can be improved.

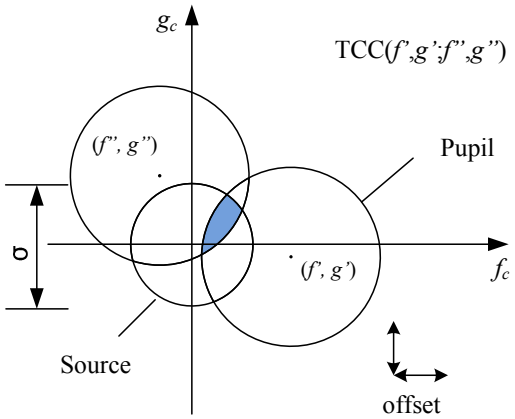

Figure 2. The intersection region of the source and two offset pupils for integration of TCC. The value of $TCC(f', g'; f'', g'')$ corresponds to the two offset pupil functions $H(f', g')$ and $H^*(f'', g'')$ and can be calculated through integration.

2.3 Analytical algorithm

TCC is essentially a double integral in most cases, and we have to use a numerical algorithm to perform the integration. However, it becomes a simple area calculation for binary sources of in-focus systems with no aberration. It is possible to use analytical methods to calculate the area through Green's theorem, since the boundary of the region is made up of several circular arcs. In the most special cases, when the mask is 1D and only 2D information of TCC is needed, the boundary of the integration region can be described analytically, and the evaluation of integration has an analytical expression. The speed and accuracy can be greatly improved in this algorithm because the integration can be avoided.

We take the calculation of TCC for 1D mask while TCC is 2D as an example to show the convenience of this algorithm. The analytical algorithm can also be applied to 4D TCC matrix computation but is much more complicated, since more possibilities have to be considered. In 2D TCC calculation, three kinds of possibilities have to be considered for area calculation considering the symmetrical characteristic of the TCC matrix and they are enumerated in Figure 3. In all of these possibilities, the area of the intersection can be transformed to a common case, which is the intersection of two circles. The integration shown in Figure 3 (a) and (b) can be calculated directly through the common case, while (c) is equal to a simple transformation.

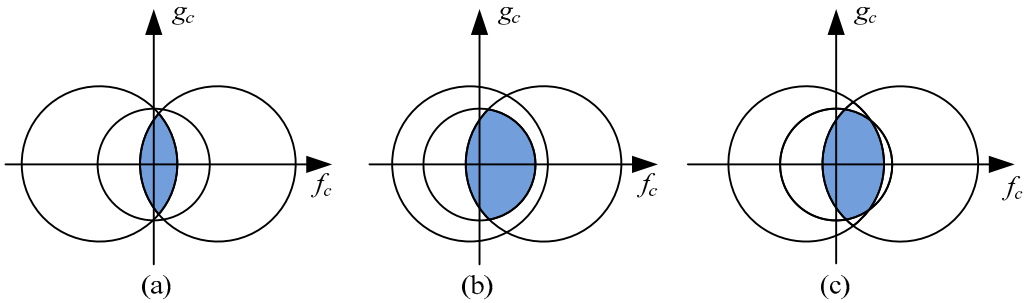

Figure 3. Three possibilities for 2D TCC calculation with the analytical algorithm. The shadow area of (a) and (b) can be calculated using the common case directly, while the shadow area in (c) equals to the difference between the sum of the source overlapping two pupils respectively and the source itself.

The area calculation of the common case in which two circles intersect is shown in Figure 4. In this case, the intersection region of two circles shown in shadow is $A(r_1, r_2, d)$, where r_1, r_2 is the radius and d is the distance between their centers.

This region can be divided into two parts. Each of them is the difference between the area of a sector and a triangle, which can be calculated analytically as:

$$\begin{aligned}
&\theta_1 = \arccos(r_1^2 + d^2 - r_2^2)/2dr_1 \\
&\theta_2 = \arccos(r_2^2 + d^2 - r_1^2)/2dr_2 \\
&c = r_1 * \sin\theta_1 \ or \ r_2 * \sin\theta_2 \\
&A(r_1, r_2, d) = A_1 + A_2 = (r_1^2\theta_1 - cd_1) + (r_2^2\theta_2 - cd_2) = r_1^2\theta_1 + r_2^2\theta_2 - cd
\end{aligned} \tag{9}$$

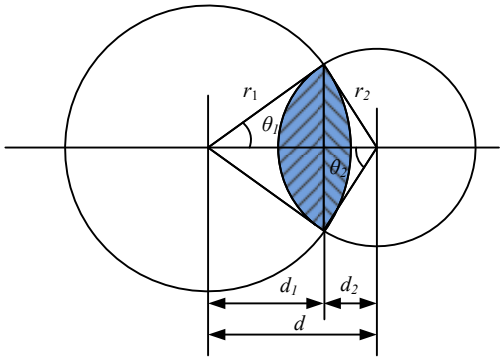

Figure 4. The area calculation of the intersection of two circles has analytical expression so we need not use integration to calculate TCC. The radiuses of the two circles are r_1 and r_2 respectively, and the distance of these two circles is d.

This algorithm can be also applied to an annular source, which is the difference of two circular sources of different σ as shown in Figure 5. As the algorithm uses analytical expressions to calculate the area and to avoid the integration, the speed and accuracy can be greatly improved. The results of this algorithm can be considered as the reference for the result of TCC calculation. However, it is only suitable for in-focus optics with no aberration where the integration can be considered as area calculation.

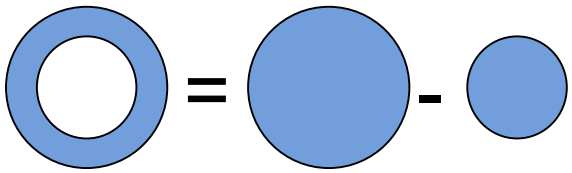

Figure 5. Annular source can be considered as the difference of two conventional sources, and we can use the analytical algorithm to calculate the TCC matrix for annular source.

2.4 FFT algorithm

While the expression of TCC is a double integral over three functions, it can be treated as a generalized convolution in frequency domain. Based on the theorem of Tichmarch, the convolution can be efficiently evaluated through the Fourier transform introduced from signal processing.

Supposing $h(x_1, y_1)$ be the inverse Fourier transform (IFT) of the pupil function given in equation (6), and $h^*(x_2, y_2)$ is its complex conjugate, we have the following formulas:

$$\begin{aligned}
H(f_c + f', g_c + g') &= \iint h(x_1, y_1)\exp[i2\pi x_1(f_c + f') + i2\pi y_1(g_c + g')]dx_1dy_1 \\
H^*(f_c + f'', g_c + g'') &= \iint h(-x_2, -y_2)^*\exp[+i2\pi x_2(f_c + f'') + i2\pi y_2(g_c + g'')]dx_2dy_2
\end{aligned} \tag{10}$$

By substituting equation (10) into the TCC formula given in equation (4), we can obtain:

$$TCC(f',g';f'',g'') = \int\cdots\int A(f_c,g_c)h(x_1,y_1)\exp[i2\pi x_1(f_c+f')+i2\pi y_1(g_c+g')]dx_1dy_1 \\ \times h^*(-x_2,-y_2)\exp[i2\pi x_2(f_c+f'')+i2\pi y_2(g_c+g'')]dx_2dy_2df_cdg_c \tag{11}$$

On the other hand, the inverse Fourier transform of the source can be written as

$$a(x,y) = \iint A(f_c,g_c)\exp[-i2\pi(f_cx+g_cy]df_cdg_c \tag{12}$$

So the expression of $a(-x_1, -y_1; -x_2, -y_2)$ is just one part of equation (11). By changing the order of integration, the evaluation of the TCC matrix can be rewritten as

$$TCC(f',g';f'',g'') = \iint\iint tcc(x_1,x_2;y_1,y_2)\exp[i2\pi(x_1f'+x_2f''+y_1g'+y_2g'')]dx_1dx_2dy_1dy_2 \tag{13}$$

$$tcc(x_1,y_1;x_2,y_2) = a(-x_1-x_2,-y_1-y_2)h(x_1,y_1)h^*(-x_2,-y_2) \tag{14}$$

From the derivation above, we obtain TCC in the spatial domain which is $tcc(x_1, y_1; x_2, y_2)$. We can calculate the spatial TCC first and then perform FT to obtain the frequency TCC, and this process is shown in Figure 6. This algorithm is based on the matrix treatment of the three functions and all of the three functions need to be discrete for matrix calculation. The functions can be sampled to get the matrix and then perform discrete Fourier transforms (DFT) for the computation of TCC. These functions are considered as periodic and the simulation range and resolution of these three functions should be the same as that of the diffraction orders of the mask.

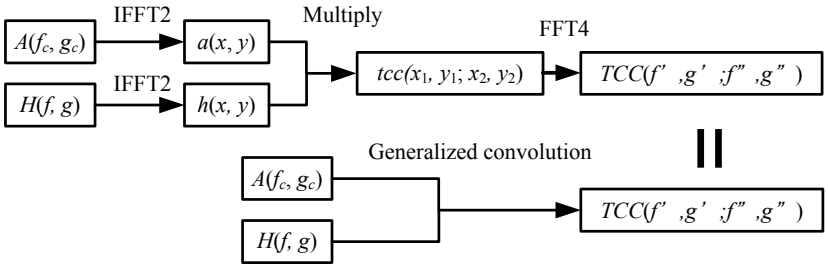

Figure 6. The integration of TCC in the frequency domain becomes multiplication in the spatial domain so that the amount of computation is greatly reduced. The speed of TCC calculation can be improved through Fourier transform.

It is noted that the spatial TCC equation is simple multiplication instead of integration in frequency domain. The speed can be greatly improved since integration is avoided, and DFT can be performed through fast Fourier Transform (FFT) in popular signal processing toolboxes. The accuracy of TCC is heavily dependent on the resolution of source in the simulation. However, we can use decimation to calculate the TCC with a resolution lower than that of the source so that the TCC resolution is not coupled with the source resolution.

3. SIMULATIONS

3.1 Results of TCC calculation

We simulated the process of TCC calculation using several mainstream sources and pupil configurations commonly used in modern lithographic tools. The results of 2D TCC are presented instead of 4D TCC for convenience, which can be shown as a 2D image. The results of optical systems both with aberration and without aberration have been obtained based on the algorithms in Section 2. Different algorithms are used based on different configurations. For in-focus systems without aberration, there are mainly four kinds of illumination settings, which are conventional, annular, dipole and quadrupole in lithographic tools. The analytical algorithm is used for TCC computation with conventional and annular sources, and the FFT algorithm is used for the other two kinds of sources. The simulation results are depicted in Figure 7, in which the wavelength is 193nm and the numerical aperture (NA) is 0.60. The TCC sampling rate is set to 64. For the FFT algorithm, a larger sampling rate consisting of 256 points on the source is used so that the source can be represented more accurately.

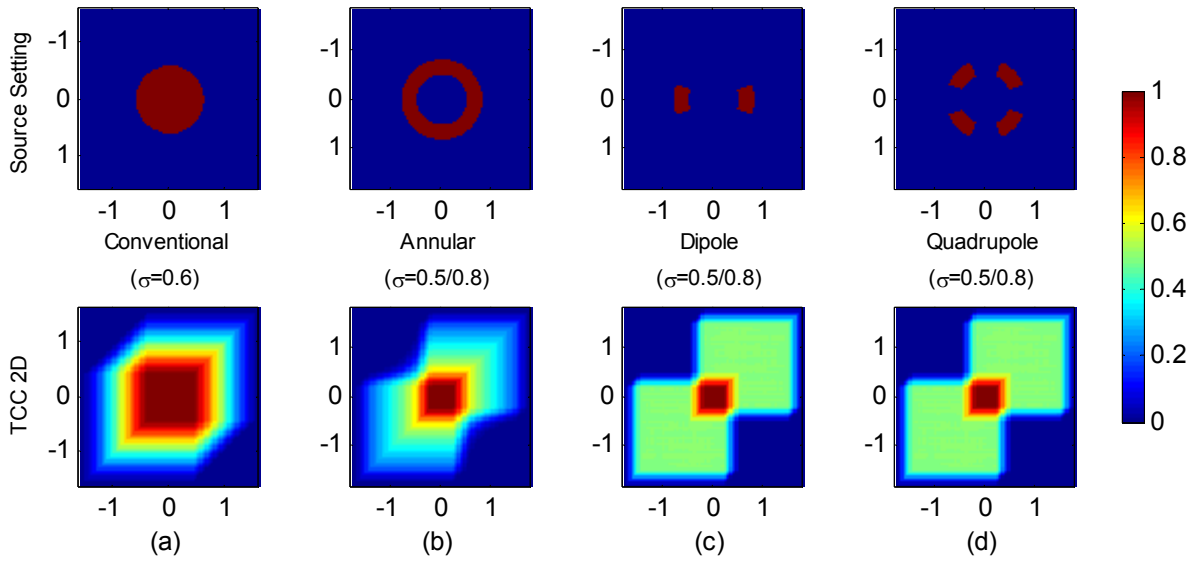

Figure 7. The simulation results of TCC for different illumination settings, including (a) conventional, (b) annular, (c) dipole, and (d) quadrupole sources. The upper charts show the illumination sources and the lower ones are 2D TCCs.

For defocused or aberrated systems, the elements of the TCC matrix are complex since the integrand with aberrated pupil is a complex function. In this situation, the analytical algorithm is not suitable for the evaluation of TCC because the integration cannot be considered as area calculation. So we can use the direct integration algorithm or the FFT algorithm for simulation. The simulation results are presented in Figure 8, including the aberration input with both odd aberration Z7 and even aberration Z9 and the two kinds of aberration together. The real parts and imaginary parts of the TCC matrix are depicted on the middle and lowest figures, respectively.

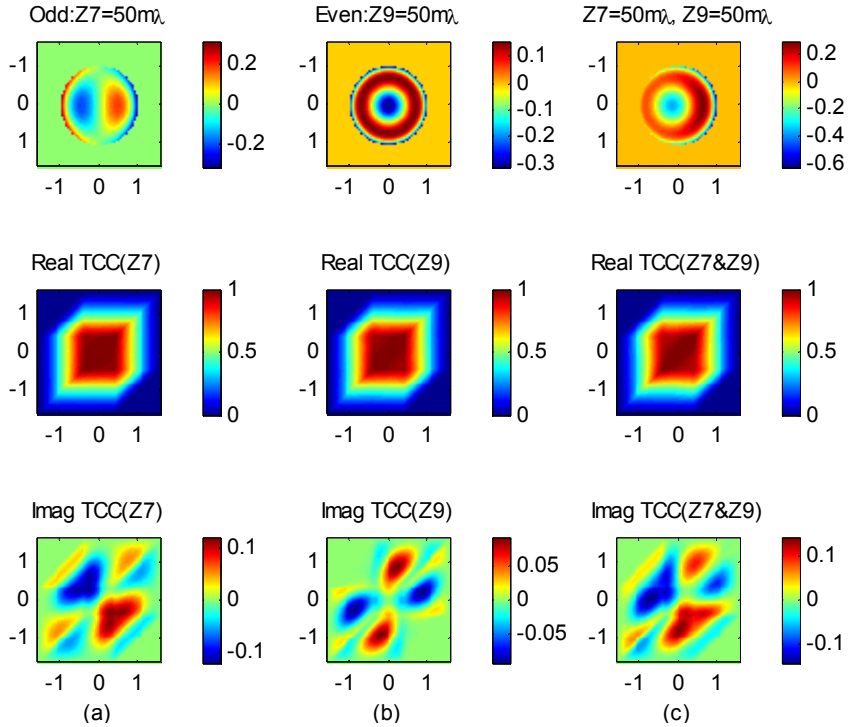

Figure 8. The simulation results of TCC for aberrated optics. The upper charts are the phase of the aberrated pupils, while the middle and lower charts are the real and imaginary parts of the TCC matrices, respectively.

3.2 Comparison of speed and accuracy

Speed and accuracy are both critical in lithographic simulation. In the theories and simulations presented above, three algorithms can be used in TCC calculation and we have analyzed the speed and accuracy theoretically. Now we intend to perform simulations to show the actual accuracy and speed of these algorithms and find the most important factor that influences the accuracy and speed of the algorithm. The speed and accuracy of these algorithms are compared so that we can find a suitable algorithm for specific optical systems in lithographic simulation.

Two important factors, which are the sampling rate of the source and the TCC resolution, determine the accuracy and speed of the algorithms based on our analysis. To show the actual relationship of the TCC with these two important factors, we performed simulations on the same optical parameters with different source sampling rates (in Figure 9) and TCC resolutions (in Figure 10). Since the analytical algorithm is only suitable for circular or annular sources without defocus and aberration, a conventional source with σ=0.65 was chosen for our simulation. In the accuracy comparison, the result by the analytical algorithm is set as the reference. The average error and max error compared with the analytical results of the two other algorithms are calculated in the simulations.

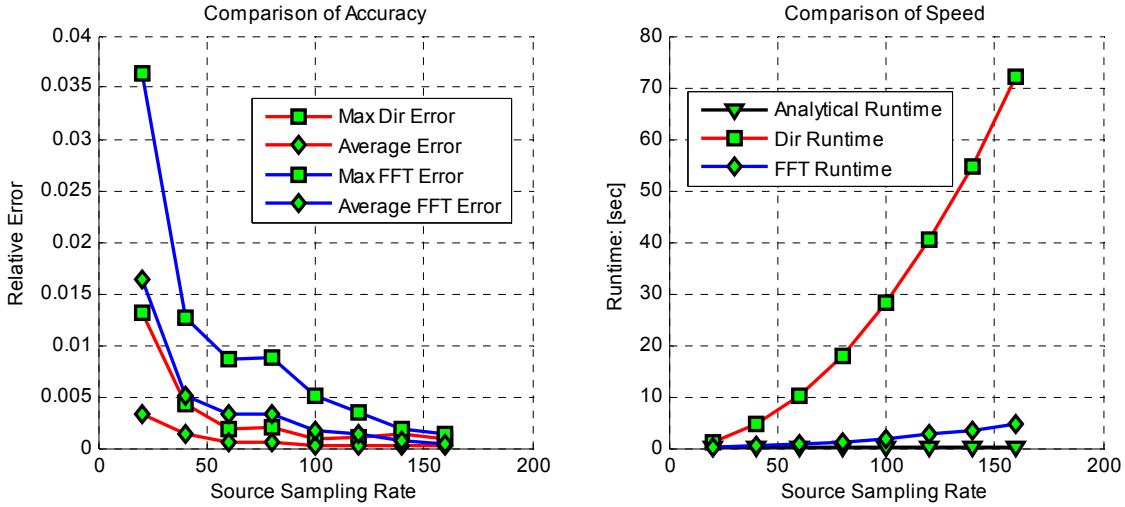

Figure 9. The relationship between the accuracy and speed of TCC and Source sampling rate. The source resolution has no influence on the accuracy of the analytical algorithm but determines the accuracy of the other two algorithms. The runtime of the two algorithms increases along with the source sampling rate.

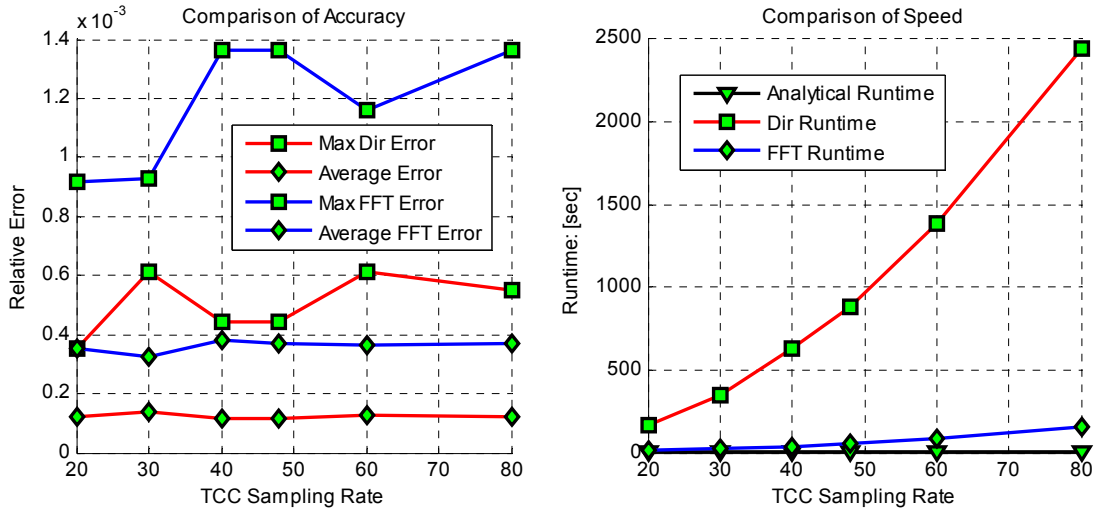

Figure 10. The relationship between the accuracy and speed of TCC and TCC sampling rate. The analytical algorithm takes little time in the simulation. For the other two algorithms, the accuracy of TCC does not change much with the same source resolution while the runtime increases quickly when the grid size of TCC increases.

From Figures 9 and 10, it is noted that the analytical algorithm takes much less time than the other two algorithms. It will be very favorable in lithographic simulation if it would be suitable for other optical systems since it is quite accurate at the same time. For the other two algorithms, the TCC resolution has little influence on the accuracy, but the runtime increases quickly as the TCC sampling rate increases. The source sampling resolution is the most important factor that influences the accuracy of the TCC. We can achieve the needed accuracy for aerial image calculation if the source sampling rate is high enough, but the speed slows down at the same time.

Based on these results we can conclude that the analytical algorithm is the most efficient and accurate algorithm, but it is only suitable for in-focus systems without aberration. The FFT algorithm is faster than the integration algorithm for the same source and TCC resolution, but the accuracy is a little lower in the simulation of 2D TCC computation. We can choose either of them when the analytical algorithm is unsuitable for the given optical systems. As for the 4D TCC computation, the runtime of the FFT algorithm remains the same as that for the 2D TCC computation, but the runtime of the integration algorithm increases significantly as the integration process has to be performed a number of times, thus we can choose the FFT algorithm for the 4D TCC computation.

4. CONCLUSIONS

In this paper, three kinds of algorithms for TCC calculation are reviewed for their rigorous formulations, physical interpretations and numerical implementations. The accuracy and speed achievable using these algorithms are compared by simulations for several mainstream illumination sources commonly used in current lithographic tools. It is noted that the integration algorithm is computationally expensive and requires a large amount of memory, especially for high resolution TCC, yet it is suitable for arbitrary imaging systems with the accuracy dependent of the numerical integration method. The analytical algorithm is an efficient one especially for in-focus imaging simulation, but it cannot be extended to optical systems with aberrations. The FFT algorithms can calculate TCC through the Fourier transform very efficiently for arbitrary imaging systems, but the accuracy is greatly influenced by the source representation methods and discrete Fourier transform algorithms. The comparison result demonstrates that each TCC calculation algorithm has its pros and cons with a compromise necessary to achieve a balance between the accuracy and speed. In practical aerial simulation, we can choose a suitable algorithm for TCC calculation. In 2D TCC matrix calculation, the analytical algorithm can be used since it can achieve a better accuracy and is also very efficient if it is available. The integration algorithm and FFT algorithm can be used in other kinds of optical systems. For the 4D TCC calculation, the FFT algorithm is better since it avoids the integration with fast matrix treatment and is suitable for any specific optical systems.

ACKNOWLEDGEMENTS

This work was supported by National Natural Science Foundation of China (Grant No. 91023032, 51005091, 50775090), National Hi-Tech Research and Development Program of China (Grant No. 2006AA04Z325), and Program for New Century Excellent Talents in University of China (Grant No. NCET-06-0639).

REFERENCES

[1] H. Hopkins, “On the diffraction theory of optical images,” Proc. R. Soc. A **217**, 408-432 (1953).
[2] M. Born and E. Wolf, Principles of Optics, 7th edition, (Pergamon, 1999), chap. 9.
[3] A. K. Wong, Optical Imaging in Projection Microlithography, (SPIE, 2005), chap 8.
[4] Y. C. Pati and T. Kailath, “Phase-shifting masks for microlithography: automated design and mask requirements,” J. Opt. Soc. Am. A **11**, 2438-2452 (1994).
[5] N. B. Cobb, “Fast optical and process proximity correction algorithms for integrated circuit manufacturing,” Ph.D. dissertation (University of California, Berkeley, 1998).
[6] E. Kintner, “Method for the calculation of partially coherent imagery,” Appl. Opt. **17**, 2747-2753 (1978).
[7] S. Subramanian. “Rapid calculation of defocused partially coherent images.” Appl. Opt. **20**, 1854-1857 (1981).
[8] R. L. Gordon, “Exact computation of scalar 2D aerial imagery,” Proc. SPIE **4692**, 517-528 (2002).
[9] R. L. Gordon and A. E. Rosenbluth, “Lithographic image simulation for the 21st century with 19th-century tools,” Proc. SPIE **5182**, 73-87 (2004).
[10] K. Yamazoe. “Computation theory of partially coherent imaging by stacked pupil shift matrix,” J. Opt. Soc. Am. A **25**, 3111-3119 (2008).

[11] R. Köhle. “Fast TCC algorithm for the model building of high NA lithography simulation,” Proc. SPIE **5754**, 918-929 (2004).
[12] R. Barakat, “Partially coherent imagery in the presence of aberrations,” Opt. Acta **17**, 337-347 (1970).
[13] M. Yeung, “Modeling aerial images in two and three dimensions,” Proc. Kodak Microelectr. Semmar. Integface **85** 115-126 (1986).
[14] P. Yu, W. Qiu, and D. Z. Pan, “Fast lithography image simulation by exploiting symmetries in lithography systems,” IEEE Trans. Semicond. Manuf. **21**, 638-645 (2008).